Journal for ImmunoTherapy of Cancer

Immune profiling of uveal melanoma identifies a potential signature associated with response to immunotherapy

Yong Qin ,[1] Kathryn Bollin,[2] Mariana Petaccia de Macedo,[3] Fernando Carapeto,[3] Kevin B Kim,[4] Jason Roszik,[5] Khalida M Wani,[3] Alexandre Reuben,[6] Sujan T Reddy,[7] Michelle D Williams,[8] Michael T Tetzlaff,[3,8] Wei-Lien Wang,[3,8] Dan S Gombos,[9] Bita Esmaeli,[10] Alexander J Lazar,[3,8] Patrick Hwu ,[5] Sapna P Patel [5]

To cite: Qin Y, Bollin K, de Macedo MP, *et al*. Immune profiling of uveal melanoma identifies a potential signature associated with response to immunotherapy. *Journal for ImmunoTherapy of Cancer* 2020;**8**:e000960. doi:10.1136/jitc-2020-000960

► Additional material is published online only. To view, please visit the journal online (http://dx.doi.org/10.1136/jitc-2020-000960).

Accepted 27 October 2020

For numbered affiliations see end of article.

Correspondence to
Dr Sapna P Patel;
sppatel@mdanderson.org

ABSTRACT

Background To date, no systemic therapy, including immunotherapy, exists to improve clinical outcomes in metastatic uveal melanoma (UM) patients. To understand the role of immune infiltrates in the genesis, metastasis, and response to treatment for UM, we systematically characterized immune profiles of UM primary and metastatic tumors, as well as samples from UM patients treated with immunotherapies.

Methods Relevant immune markers (CD3, CD8, FoxP3, CD68, PD-1, and PD-L1) were analyzed by immunohistochemistry on 27 primary and 31 metastatic tumors from 47 patients with UM. Immune gene expression profiling was conducted by NanoString analysis on pre-treatment and post-treatment tumors from patients (n=6) receiving immune checkpoint blockade or 4-1BB and OX40 dual costimulation. The immune signature of UM tumors responding to immunotherapy was further characterized by Ingenuity Pathways Analysis and validated in The Cancer Genome Atlas data set.

Results Both primary and metastatic UM tumors showed detectable infiltrating lymphocytes. Compared with primary tumors, treatment-naïve metastatic UM showed significantly higher levels of CD3+, CD8+, FoxP3+ T cells, and CD68+ macrophages. Notably, levels of PD-1+ infiltrates and PD-L1+ tumor cells were low to absent in primary and metastatic UM tumors. No metastatic organ-specific differences were seen in immune infiltrates. Our NanoString analysis revealed significant differences in a set of immune markers between responders and non-responders. A group of genes relevant to the interferon-γ signature was differentially up-expressed in the pre-treatment tumors of responders. Among these genes, suppressor of cytokine signaling 1 was identified as a marker potentially contributing to the response to immunotherapy. A panel of genes that encoded pro-inflammatory cytokines and molecules were expressed significantly higher in pre-treatment tumors of non-responders compared with responders.

Conclusion Our study provides critical insight into immune profiles of UM primary and metastatic tumors, which suggests a baseline tumor immune signature predictive of response and resistance to immunotherapy in UM.

BACKGROUND

Uveal melanoma (UM) is a rare disease in which cancer cells derive from melanocytes within the uveal tract of the eye. It is the most common primary intraocular malignancy in adults and comprises about 5% of all melanomas. Approximately 50% of patients diagnosed with primary UM will develop metastatic disease,[1] with the liver being the most common site involved. Patients with metastatic UM present a median overall survival (OS) of 6 to 12 months.[1] It is also known that UM harbors a unique molecular signature, distinct from that of cutaneous melanoma (CM). For example, *BRAF* and *NRAS* mutations commonly detected in CM, rarely appear in UM,[2 3] while *GNAQ* and *GNA11* mutations are found in approximately 80% of UM.[3] Furthermore, UM has a lower mutational load compared with CM, which could also contribute to its low tumor immunogenicity.[4 5]

To date, no systemic therapy has demonstrated improved clinical outcomes in UM patients, with most drugs used to treat metastatic CM, proving mostly ineffective in the UM setting.[6 7] Targeted therapy trials for advanced uveal melanoma have fallen short with other therapies such as the MEK1/2 inhibitors selumetinib and trametinib.[8] Although immunotherapy has shown promise for metastatic CM, checkpoint inhibitors, such as ipilimumab and tremelimumab, have shown limited clinical efficacy (<10%) with no true benefit to OS for advanced UM patients in clinical trials.[9 10] Checkpoint inhibition with PD-1-blocking antibodies, such as pembrolizumab or nivolumab, have also been investigated in metastatic UM, with similar results (3 to 11%) and minimal impact on survival.[11] Notably, the low response rates and

negligible impact on survival of monotherapy checkpoint inhibition in UM sharply contrast with promising results in CM.[7 12]

The poor response to immunotherapy in UM highlights a knowledge deficit of how metastatic UM escapes immune surveillance or develops resistance. The study of this poor response mechanism was hindered by the limited number of clinical UM tumors treated with immunotherapy available for research. Thus, there is a critical need to better understand physiologic immunosuppressive mechanisms in order to improve treatment options for patients with UM. To date, there is a paucity of studies characterizing the immune infiltrate of metastatic UM tumors. In a previously published pilot study, we described the immune profile of metastatic UM compared with metastatic CM. It was revealed that UM was deficient in tumor-infiltrating lymphocytes (TIL) compared with CM.[13] In this current study, we sought to further characterize the immune phenotypes and tumor microenvironment of UM and alternations occurring relative to therapeutic response. In this effort, we methodically analyzed key markers of immune infiltrates in primary and metastatic tumors from 47 patients with UM. Longitudinal tumor samples from a subset of patients receiving immunotherapy were evaluated.

METHODS

Patients and clinical characteristics

Based on the quality and quantity of available formalin-fixed paraffin-embedded (FFPE) tumor tissues, 47 patients with UM treated at The University of Texas MD Anderson Cancer Center (MDACC) between 2011 and 2016 were selected for immunohistochemistry (IHC) staining and analysis study of immune infiltrates. All patients provided written consent for research tissue banking and analysis. Archived FFPE tissue from 27 primary and 31 metastatic samples from 47 unique UM patients were utilized for this study. The data regarding treatment exposure and anatomic sites are available for all cases. The clinical characteristics for the patients, including the metastatic sites, are shown in table 1. The detailed characteristic information of all primary tumors is shown in online supplemental table S1. The treatment information for relevant metastatic samples is shown in online supplemental table S2.

Longitudinal gene expression profiling was conduc a cohort of six patients with UM who received immunotherapy at Scripps MD Anderson, California Pacific Medical Center, and MDACC. The patient from Scripps MD Anderson was treated with ipilimumab plus nivolumab, and the other patient from California Pacific Medical Center was treated with OX40 agonist plus 4-1BB agonist. Both patients were characterized as responders. Four patients from MD Anderson were characterized as non-responders, all treated with monotherapy checkpoint blockade (anti-PD-1, anti-PD-L1, or anti-CTLA-4 antibody) at MDACC and had stable (1 out of 4) or progressive (3 out of 4) disease. The characteristics of these six patients with UM who received immunotherapy are listed in online supplemental table S3.

Immunohistochemistry and digital image analysis

An H&E section was manufactured from each UM FFPE block and reviewed by a pathologist to ensure the presence of viable tumor and selection of the best representative block when multiple blocks were available for the same sample. Additional sections of 4 µm thickness were cut from the FFPE block for IHC staining and analysis. Samples with high melanin content were submitted to 24-hour bleaching with hydrogen peroxidase at room temperature prior to IHC staining. IHC staining was performed in a Leica Bond Max automated stainer (Leica Biosystems, Buffalo Grove, Illinois) using antibodies against CD8 (clone C8/144B, Thermo Scientific, Waltham, Massachusetts) at a dilution of 1:25, PD-L1 (clone E1L3N, Cell Signaling, Danvers, Massachusetts) at a dilution of 1:100, PD1 (Clone- EPR4877, Abcam) at a dilution of 1:25, CD3 (clone A0452, Agilent Technologies, Santa Clara, California) at a dilution of 1:100, CD68 (clone PG-M1, Agilent Technologies, Santa Clara, California) at a dilution of 1:450, and FoxP3 (clone 206D, Biolegend, San Diego, California) at a dilution of 1:50. All stains were performed under optimized conditions and included a positive control (human lymph node) and a negative control without the primary antibody, as described previously.[13] The Leica Bond Polymer Refine Detection kit (Leica Biosystems) was used for detection with diaminobenzidine (DAB) used as the chromogen. All slides were counterstained with hematoxylin and scanned into a digital pathology slide scanner and analyzed using the Aperio analysis software (Aperio AT Turbo, Leica Biosystems). From each sample, one to five 1 mm^2 areas were randomly selected within the tumor architecture by a pathologist for quantification, depending on the size of the tumor. CD3, CD8, CD68, FoxP3, PD-1 was evaluated using the nuclear algorithm to identify lymphoid cells vs tumor cells and the data retrieved as the number of positive inflammatory cells per the analyzed area and normalized as counts/mm^2. PD-L1 was evaluated as the percentage of cell positive. It was challenging for IHC analysis in some of the small biopsy UM tumors collected in our study. Due to inadequate tumor sampling, some tumors did not have sufficient samples to analyze all listed immune markers.

All the IHC staining and whole H&E sections of tumor samples were reviewed and analyzed by two pathologists, WLW and FC, independently. After review, the best representative areas were punched twice by a 1 mm needle to form a tissue microarray block. Then, the selected tumor tissues were subject to further analyzes to review the lymphocytic location once by checking the respective H&E sections. The location of lymphocytic infiltrate was categorized as: (a) intratumoral: when the lymphocytes are distributed diffusely inside the tumor mass and (b) peri-tumoral:

Table 1 Patient and tissue characteristics

	Primary	Metastatic	Total
Patient Number	n=26	n=31	n=47
Gender—no. of patients (%)			
Female	13 (50)	16 (51.6)	29 (61.7)
Male	13 (50)	15 (48.4)	18 (48.3)
Age—years			
Range	40 to 82	28 to 78	28 to 82
Median	70	64	65
	Primary	**Metastatic (treatment-naïve)**	**Metastatic (on/post treatment)**
Biopsy site—no. of patients (%)			
Tissue number	n=27	n=29	n=28
Eye (primary tumors)	27 (100)		
Liver (metastatic tumors)		18 (62.1)	8 (28.6)
Lung (metastatic tumors)		6 (20.7)	2 (10.7)
Soft tissue and others (metastatic tumors)		5 (17.2)	17 (60.7)
CD8+ cells/mm^2			
Range	0 to 992.02	4.16 to 1990.7	1.30 to 2011.9
Median (SD)	47.44 (326.09)	361.4 (452.84)	212.4 (530.44)
CD3+ cells/mm^2			
Range	1.6 to 1185.27	39.40 to 1371.5	6.73 to 3174.4
Median (SD)	87.79 (413.83)	326.97 (397.26)	164.2 (709.27)
CD68+ cells/mm^2			
Range	0 to 618.57	1.27 to 3604.2	0.63 to 2386.6
Median (SD)	81.67 (198.35)	266.18 (763.39)	330.06 (606.22)
FOXP3+ cells/mm^2			
Range	0.61 to 57.96	0.61 to 248.41	0 to 402.32
Median (SD)	8.20 (18.17)	25.76 (71.79)	31.07 (101.97)
CD4+ cells/mm^2			
Range	1.01 to 862.82	4.41 to 1047.91	5.03 to 1224.16
Median (SD)	31.91 (194.84)	110.05 (273.70)	87.28 (311.43)
PD-1+ cells/mm^2			
Range	0 to 153.18	0 to 276.65	0 to 327.89
Median (SD)	1.60 (30.17)	3.60 (58.18)	3.93 (82.28)

SD, Standard deviation

.

lymphocytes occurring mostly in the tumor stroma or surrounding the tumor but not in direct contact with tumor cells.

Gene expression profiling

NanoString was performed on the pre-treatment and post-treatment of immunotherapy cohort using the nCounter PanCancer Immune Profiling codeset (NanoString) of 770 cancer-related and immune response genes (online supplemental table S4). RNA was extracted using the Highpure miRNA isolation kit (Roche) from FFPE blocks, following initial confirmation of tumor presence and content by two pathologists by H&E. For gene expression studies, 1 µg of RNA was used per sample. Hybridization was performed for 16 to 18 hours at 65°C and loaded onto the nCounter Prep Station for binding and washing prior to scanning and by the capture of 600 fields using the nCounter.

Statistical analysis

Statistical analysis was performed with GraphPad Prism V.6.0 (La Jolla, California). Unpaired non-parametric t-tests were performed to compare the levels of tested immune markers in UM tumors. The level of statistical significance was set as 0.5.

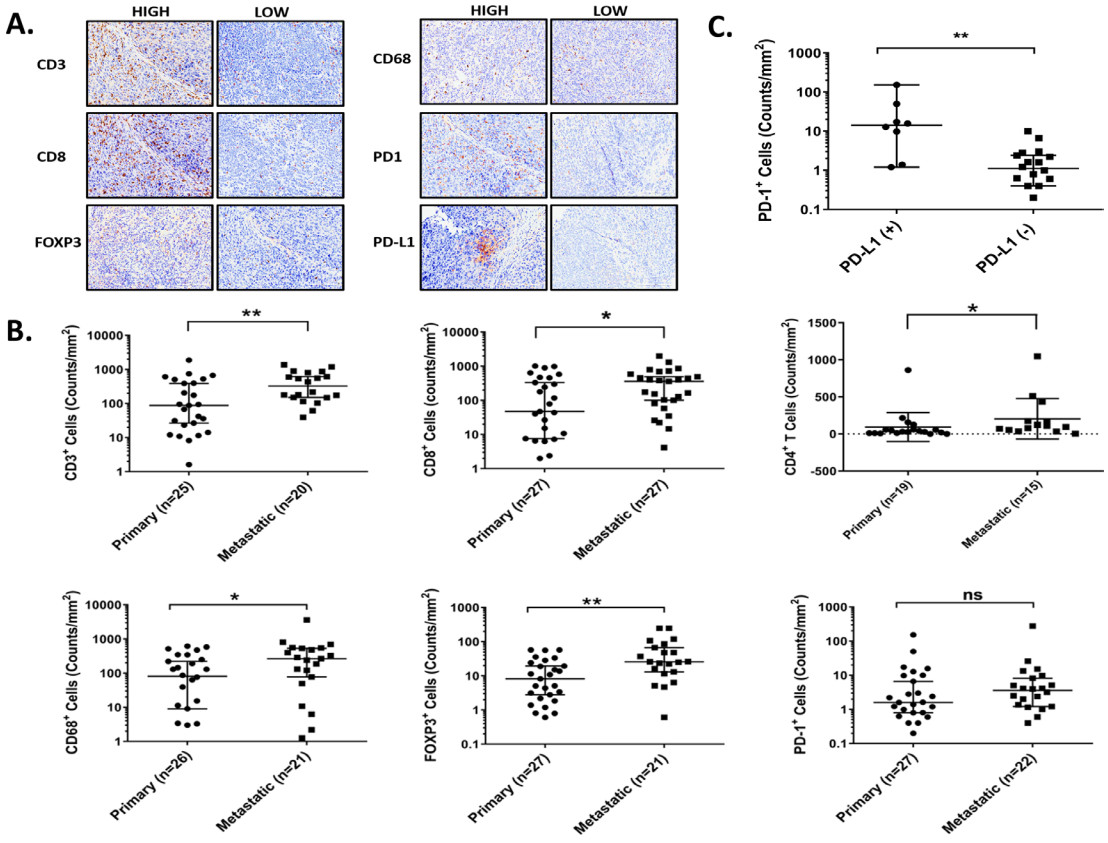

Figure 1 Immune infiltrates and PD-L1 expression in primary and metastatic uveal melanoma. (A) Representative immunohistochemistry staining for CD3, CD8, CD68, FoxP3, PD-1, and PD-L1 in uveal melanoma (UM) tumor tissues. positive staining denoted by brown/red color. (B) Comparison of immune infiltrate in UM primary and metastatic tumors by quantification of CD3+, CD8+, CD4+, CD68+, FoxP3+, and PD-1+ infiltrates in 27 primary tumors and 29 metastases. (C) Comparison of PD-1+ infiltrate levels between PD-L1-positive and PD-L1 negative primary UM tumors. *=p<0.05; **=p<0.001; ns=not significant.

RESULTS

Immune infiltrates in UM tumors

There were 27 primary tumors from 26 patients (two tumor samples were collected from one patient with local recurrence in the orbit), which showed positive staining for CD3 (100%, median: 87.79 /mm^2, 1.61 to 1185.27/mm^2), CD8 (96.3%, median: 47.44 /mm^2, 0 to 992.02/mm^2), and CD68 (88.5%, median: 81.67/mm2 0 to 618.57/mm2) (figure 1A)). All tested primary UMs showed positive staining of FoxP3 Treg, with a median of 8.20 FoxP3$^+$ cells /mm^2 (0.61 57.96/mm2, table 1). The total lymphocyte population, denoted by CD3 stain, is mainly comprised of CD8 T cells and CD4 T cells. Therefore, we estimated CD4 expression by subtracting the proportion of CD8 T cells from the total CD3 population. The estimated CD4+ infiltrates in tested primary tumors showed a median of 31.91 CD4+ cells/mm^2 (1.01 to 862.82/mm^2, table 1).

CD3+, CD8+, CD68+, and FoxP3+ infiltrates were detected in all available treatment-naïve metastatic UM tumors (table 1). Moreover, treatment-naïve metastatic tumors showed significantly higher levels of CD3+ (median: 326.97/mm^2, 39.40 to 1371.5/mm^2, p=0.0059), CD8+ (median: 361.4/mm^2, 4.16 to 1990.7/mm^2, p=0.0423), and FoxP3+ (median: 25.76/mm^2, 0.61 to 248.41/mm^2, p=0.0028) T lymphocytes than primary tumors (figure 1B). Infiltrating CD68+ macrophages were significantly higher in treatment-naïve metastases (median: 266.18/mm^2, 1.27 to 3604.2/mm^2) than primary tumors (p=0.0424, figure 1B). The estimated CD4+ infiltrates were also significantly higher in treatment-naïve metastatic tumors (median: 110.05/mm^2, 4.41 to 1047.91/mm^2) than primary tumors (p=0.0138, figure 1B). Limited matching pairs of primary and metastatic tumors from the same patients were collected in our study. There were 11 patients with matching primary and metastatic tumors. Three of the metastases were treatment-naïve samples, with incomplete IHC data due to exhaustion of the FFPE. The other eight metastases were collected at various time points after a variety of treatments (immunotherapy, targeted therapy, and liver-directed therapy), also with incomplete IHC data due to tissue exhaustion. Due to the limited sample size, no generalizations can be made, other than metastatic tissues have higher FoxP3+ infiltrates than primary tumors from the same patient (online supplemental figure S1).

The spatial distribution of CD8+ T cells in all tumor samples was quantified based on the pathological analysis. Intratumoral CD8+ infiltrates were noted in the majority of primary UM tumors (92.6%, 25/27) and treatment-naïve metastatic tumors (79.3%, 23/29) without the presence of peritumoral infiltrates (online supplemental figure

S2). Although, a higher percentage of metastatic tumors were detected with peritumoral infiltrates, no significant differences for the peritumoral or intratumoral infiltrates were found among primary tumors, treatment-naïve, and post-treatment metastatic UM tumors (online supplemental figure S2).

We further analyzed the correlation of these T-cell markers in UM tumors. As expected, the levels of CD3 were positively correlated with CD8 or CD4 in UM primary tumors and metastases (primary: CD3 and CD8: Spearman Rho=0.93, p<0.001; CD3 and CD4: Spearman Rho=0.93, p<0.001; metastatic: CD3 and CD8: Spearman Rho=0.58, p<0.05; CD3 and CD4: Spearman Rho=0.68, p<0.05; online supplemental figure S3A). The levels of CD4 were positively correlated with CD8 in primary tumors but not in metastatic tumors (primary: CD4 and CD8: Spearman Rho=0.83, p<0.001, online supplemental figure S3A). The levels of PD-1+ T cells were also positively correlated with CD8+ density in primary tumors, but only with CD4+ density in treatment-naïve metastatic tumors (primary: PD-1 and CD8: Spearman Rho=0.42, p<0.05; metastatic: PD-1 and CD4: Spearman Rho=0.83, p<0.001, online supplemental figure S3A). Tumor-infiltrating FoxP3 +cells showed a significant positive association with the presence of CD8 +T cells in UM metastases and primary tumors (primary: Spearman Rho=0.55, p<0.01; metastatic: Spearman Rho=0.57, p<0.05, online supplemental figure S3A,B). Moreover, levels of FoxP3+ infiltrates were positively correlated with CD3+ and CD4+ density in primary UM (FoxP3 and CD3: Spearman Rho=0.66, p<0.001; FoxP3 and CD4: Spearman Rho=0.50, p<0.05, online supplemental figure S3A,B).

Low levels of PD-1 and PD-L1 expression in UM tumors

PD-L1 was negative (defined as the absence of any PD-L1 staining) in 66.4% of tested primary tumors by IHC, and, where positive, was noted in <1% of tumor cells (online supplemental table S2). Moreover, the primary UM tumors containing any amount of PD-L1+ tumor cells exhibited higher PD-1+ infiltrates (median=14.32 PD-1+/mm^2, 1.21–153.18/mm^2) than those tumors that were negative for PD-L1 expression (median=1.11 PD-1+/mm^2, 0–10.05/mm^2) (p=0.0016, figure 1C). Notably, PD-L1 expression was undetectable in all treatment-naïve metastatic UM tumors (n=29, online supplemental table S5). Low levels of infiltrating PD-1+ cells were seen in primary UM tumors (median=1.6 PD-1+/mm^2, 0 to 153.18/mm^2) and metastatic tumors (median=3.6 PD-1+/mm^2, 0 to 267.65/mm^2) with no significant difference between these two groups (figure 1B).

Immune infiltrates in UM metastases from various anatomic sites

In 29 treatment-naïve metastatic UM tumors collected in this study, 62% were liver metastases, and 38% of tumors were metastases from lung, soft tissues, skin, and subcutaneous tissue of the abdomen. We performed an analysis to compare the immune infiltrates between tumors collected from different organ sites. As shown in figure 2A, no difference was seen in levels of CD3+, CD8+, CD4+, CD68+, PD-1+, and FoxP3+ among treatment-naïve metastatic tumors from liver, lung, lymph node, soft tissue, and other organ sites.

Longitudinal immune profiling of UM patients on treatment for metastatic disease

To date, no study has analyzed the effect of systemic therapy on UM tumors' immune infiltrates. In our study, 27 metastatic UM tumors were collected from patients pre-systemic or post-systemic therapy, including 16 patients treated with targeted therapy, and 11 patients treated with monotherapy checkpoint blockade. First, we compared the immune infiltrates profiles of treatment-naïve tumors and tumors collected post or on systemic treatments. As shown in figure 2B, there was no difference for CD3+, CD8+, CD4+, CD68+, PD-1+, and FoxP3+ cells between these two groups. Next, we compared the effects of targeted and other systematic therapies with immunotherapies on the UM metastatic tumors' immune infiltrate. As shown in figure 2C, there was no difference for CD3+, CD8+, CD4+, CD68+, PD-1+, and FoxP3+ cells between these two groups. Markedly, the metastatic tumor samples from patients post or on monotherapy checkpoint blockade show numerically higher levels of immune infiltrates compared with tumors collected from patients post- or on targeted therapy. (Median: CD8, immunotherapy=343.56/mm^2 versus MEKi and others=181.85/mm^2, p=0.1523; CD3, immunotherapy=395.71/mm^2 versus MEKi and others=99.77/mm^2, p=0.0792; CD4, immunotherapy=151.0/mm^2 versus MEKi and others 63.02/mm^2, p=0.1812; CD68, immunotherapy=439.14/mm^2 versus MEKi and others=303.38/mm^2, p=0.347; FoxP3, immunotherapy=83.81/mm^2 versus MEKi and others=15.72/mm^2, p=0.072) (figure 2C).

Effects of immunotherapy on immune gene expression in UM patients

Longitudinal pre-treatment and post-treatment UM tumors were collected from six patients (n=2 responders (R) and n=4 non-responders (NR)) receiving checkpoint inhibitor immunotherapy. R tumors were derived from one patient treated with nivolumab plus ipilimumab and one patient treated with 4-1BB+OX40 dual co-stimulation. Both patients showed partial responses to treatments. NR tumors were derived from four patients treated with monotherapy checkpoint blockade (anti-PD-1, anti-PD-L1, and anti-CTLA-4 antibody) who had stable (1/4) or progressive (3/4) disease as the best response (online supplemental table S3). We performed gene expression profiling to identify gene signatures associated with the response by NanoString analysis on these tumors. The PanCancer Immune panel of 770 immune relevant genes was applied in our NanoString study. The analysis of these tumor samples showed that three genes, *NUP107*, *TANK*, and *IL12A*, were significantly higher in the post-treatment tumors compared with pre-treatment

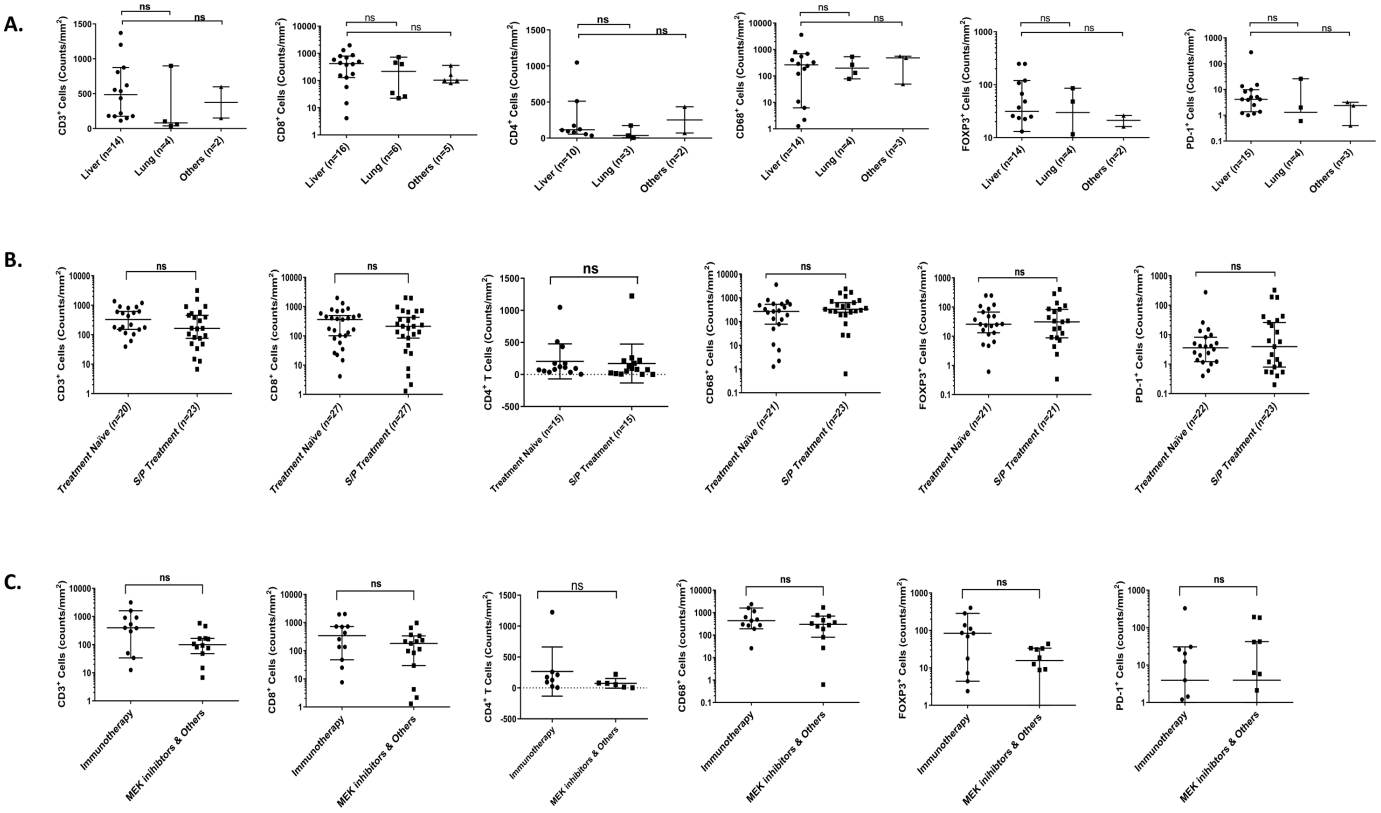

Figure 2 Quantification of immune infiltrates in metastatic uveal melanoma (UM) tumors receiving treatment. (A) comparison of immune infiltrates (CD3+, CD8+, CD4+, CD68+, FoxP3+, and PD-1+) in UM metastases by organ sites (liver, lung, and others). (B) Immune infiltrates levels in longitudinal metastatic tumor samples of UM patients on systematic therapies. (C) Comparison of immune infiltrates in UM metastases received immunotherapy or targeted therapies. ns=not significant.

samples (the difference between normalized expression in the two groups; two-sided Student's t-test p≤0.05) (figure 3A). Moreover, 10 genes, *TNFSF4*, *TIRAP*, *SBNO2*, *PIN1*, *SMAD3*, *BID*, *CDKN1A*, *MS4A1*, *MAVS*, and *CTSL*, showed significant decreases in the post-treatment tumors compared with pre-treatment samples (figure 3A).

Pre-treatment gene expression signature correlates with response to immunotherapy

We then questioned whether pre-treatment gene expression would differentiate R versus NR prior to immunotherapy. Two sets of genes were differentially expressed between response groups (figure 3B, two-sided Student's t-test p≤0.05). A set of 12 genes (*CDH1*, *HLA-DRB4*, *HLA-G*, *TLR3*, *IFITM2*, *SOCS1*, *SLAMF1*, *CASP3*, *ATF1*, *TBK1*, *CD164*, and *ITCH*) were significantly expressed higher in pre-treatment R compared with NR. Moreover, a group of 13 genes (CXCR1, CXCR2, PTGS2, NOS2A, IL4, IL17A, IL19, CCL20, IGLL1, LTK, TAB1, S100A12, and CD3EAP) were significantly higher in pre-treatment NR compared with R. Ingenuitypathway analyses (IPA) are shown for both of these gene sets in figure 3C,D). For the set of genes upregulated in the pre-treatment R, interferon (IFN)-γ was identified as the main upstream regulator for eight genes of this set based on IPA (figure 3C). Notably, most of the genes upregulated in the pre-treatment NR encoded important cytokines and molecules of the pro-inflammatory signal network regulated by IL13, IL4, and NF-κB (figure 3D).

Taking advantage of publicly available RNAseq data of pre-treatment CM tumor samples receiving anti-PD-1 therapy from previously published work,[14] we analyzed whether the gene signatures identified in UM tumors also applied to CM. *CDH1*, which was identified as one of the genes upregulated in pretreatment R UM tumors, was also found to be expressed significantly higher among R versus NR in pre-treatment CM (figure 3E).

Next, we compared the expression of immune genes of post-treatment UM tumors between R and NR. Three genes, *PRKCE*, *HMGB1*, and *CCL28*, were expressed significantly higher in the post-treatment tumors of NR compared with R (figure 4A). IPA analysis revealed that tumor necrosis factor (TNF) is a key regulator for the activation and upregulation of all three genes within the cell signaling network (figure 4B).

SOCS1 as a potential mediator in UM responding to immunotherapy

As shown in figure 3B, the mRNA levels of suppressor of cytokine signaling 1 (*SOCS1*) and major histocompatibility complex (MHC) molecules, *HLA-G* and *HLA-DRB4*, were significantly higher in pre-treatment tumors of R versus NR. Further analysis of The Cancer Genome Atlas (TCGA) data of 80 primary UM tumors showed there

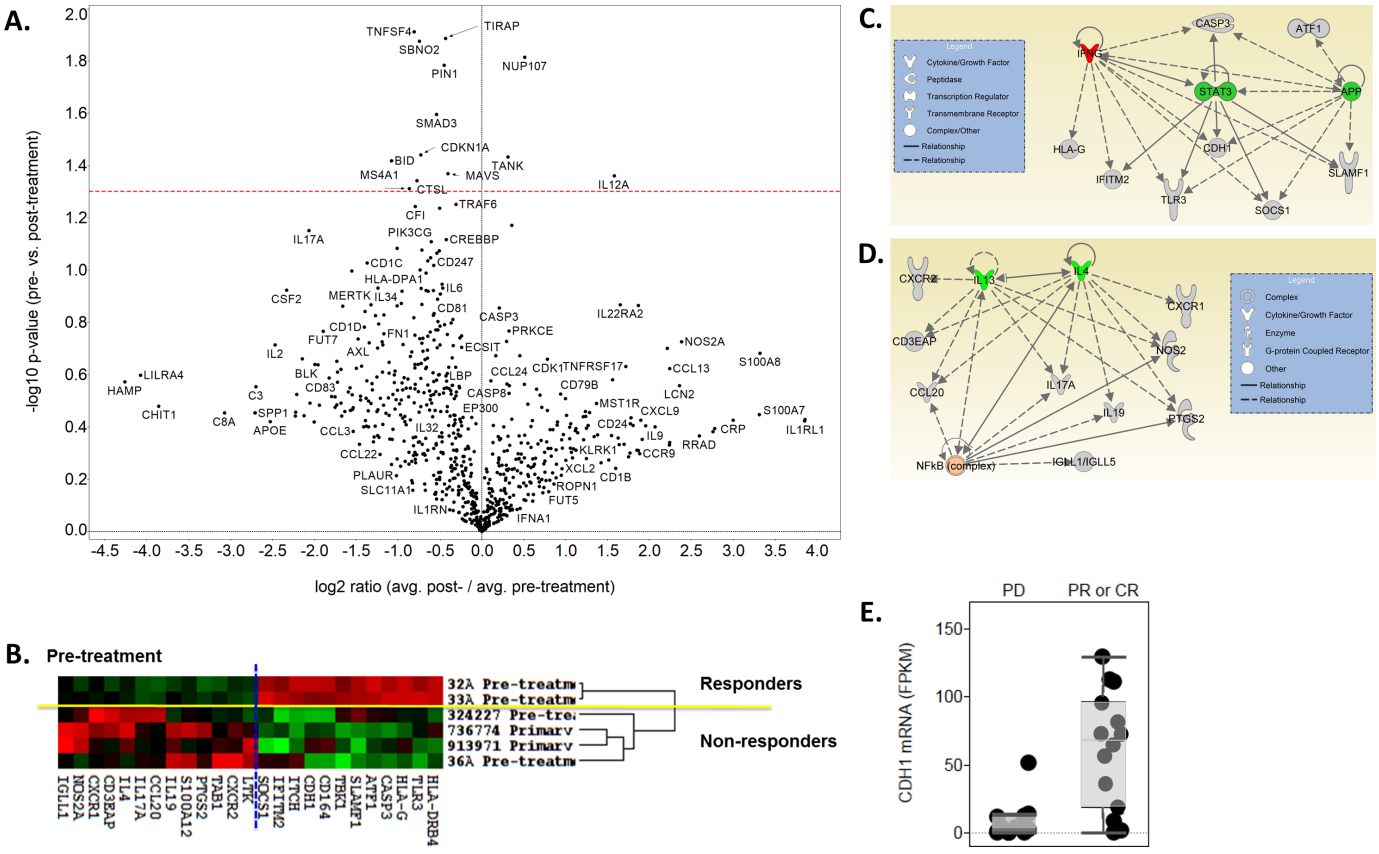

Figure 3 The analysis of matching metastatic tumors (pre-treatment and post-treatment) from six patients who received immunotherapy by NanoString. (A) Relative gene expression level change in post-treatment tumors against pre-treatment tumors. the genes above red line show significantly changes of expression levels in post-treatment tumors compared with pre-treatment tumors (p<0.05). *IL12A*, *NUP107*, and *TNAK* expressions were upregulated, and *TNFSF4*, *TIRAP*, *SBNO2*, *PIN1*, *SMAD3*, *CDKN1A*, *BID*, *MS4A1*, *CTSL*, and *MAVS* were downregulated after treatment in all six patients' um tumors. (B) Heat map demonstration of NanoString analysis of pre-treatment tumors of uveal melanoma responders (R, n=2) and non-responders (NR, n=4) to immunotherapies. two sets of genes were differentially expressed between the responding versus non-responding pre-treatment tumors (p≤0.05). (C) Functional network analysis by Ingenuity Pathways Analysis (IPA) reveals that interferon-γ is the major upstream regulator for the expression of a group of genes (*CASP3, CDH1, HLA-G, IFITM2, SLAMF1, SOCS1, TLR3, and ATF1*), which are significantly expressed at a higher level in pre-treatment tumors of responders to immunotherapy. (D) Functional network analysis by IPA reveals that proinflammatory NF-kB, interleukin (IL)-4, and IL-13 are major upstream regulators for the expression of a group of genes (*CXCR1*, *CXCR2*, *PTGS2*, *NOS2A*, *IL4*, *IL17A*, *IL19*, *CCL20*, *IGLL1*, *LTK*, TAB1, S100A*12*, and *CD3EAP*), which are significantly expressed at a higher level in pre-treatment tumors of non-responders to immunotherapy. (E) The expression of *CDH1* was significantly higher in the pre-treatment cutaneous melanoma (CM) tumors of responders compared with non-responders who received anti-PD-1 therapy. The cohort of CM tumors was derived from the published data of previous study.[14] IPA analysis: nodes represent genes, with their shape representing the functional class of the gene product (as shown in left panel). Genes with gray nodes are focused genes identified by the NanoString analysis. Genes with purple nodes are generated through the network analysis from IPA as upstream regulators for those genes in gray color. The lines between genes represent known interactions, with solid lines representing direct interactions and dashed lines representing indirect interactions.

was a significant survival disadvantage for patients whose tumors lacked SOCS1 expression (<median) compared with those with high SOCS1 expression (>median) (figure 5A). We compared *SOSC1* mRNA levels among various tumors and normal tissues based on TCGA and Genotype-Tissue Expression (GTEx) data. As shown in figure 5B, *SOCS1* mRNA levels were significantly lower in UM compared with skin melanoma and lung cancer, which are known to have a high response rate to checkpoint blockade.

Human leukocyte antigens (HLA) play crucial roles in the interaction of malignant cells with immune cells.[15] Various studies have shown that *SOCS1* regulates MHC I and II molecules levels in fibroblast and tumor cells.[16–18] In pre-treatment tumors collected from patients with UM treated with immunotherapy, R expressed higher SOCS1, HLA-DRB4, and HLA-G than NR (figure 5C). We analyzed the expression patterns of *SOCS1* and MHC I and II molecules from the UM TCGA. As shown in table 2 and figure 5D, SOCS1 mRNA levels were significantly correlated with the levels of most HLA molecules in UM tumors in the TCGA, including HLA-A, HLA-B, HLA-C, and HLA-G.

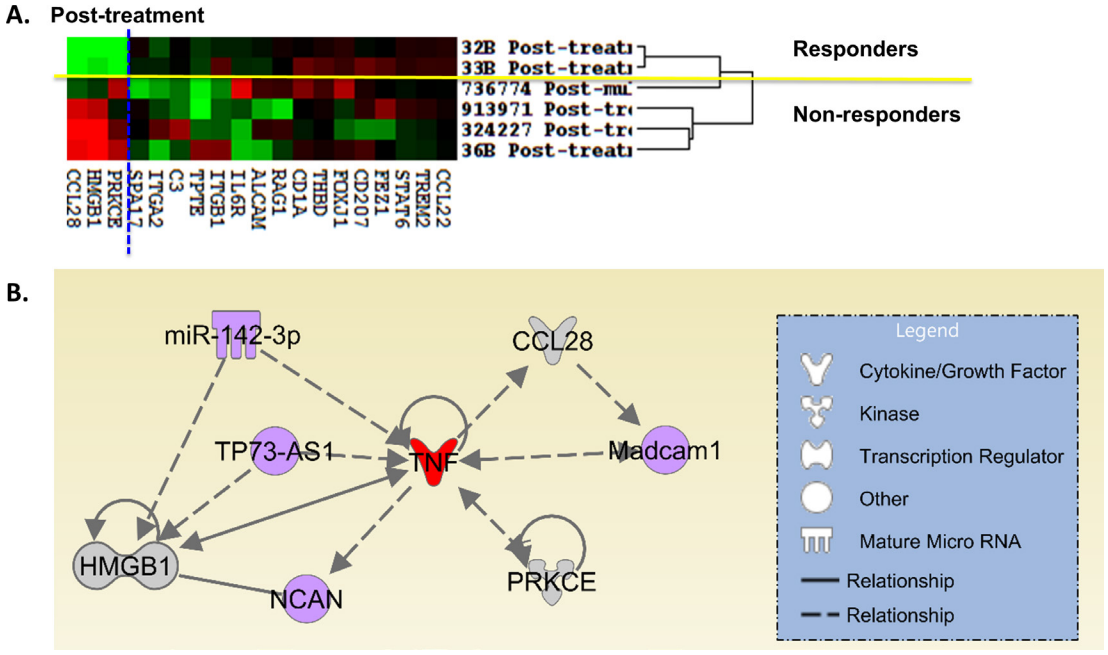

Figure 4 NanoString analysis of post-treatment tumors of uveal melanoma (UM) responders (n=4) and non-responders (n=2) to immunotherapies. (A) The heat map demonstrates that two sets of genes were differentially expressed between the responding versus non-responding post-treatment tumors (p≤0.05). (B) Functional network analysis by Ingenuity Pathway Analysis (IPA) reveals that TNF is the major upstream regulator for the expression of HMGB1, PRKCE, and CCL28, which are significantly expressed at a higher level in post-treatment tumors of non-responders to immunotherapy. Genes with gray nodes are focused genes identified by the NanoString analysis. Genes with red and purple nodes are generated through the network analysis from IPA as upstream regulators for those genes in gray color.

DISCUSSION

Our work demonstrates the presence of immune infiltrates in the majority of primary and metastatic UM tumors. In fact, 100% of all treatment-naïve metastatic tumor samples had a detectable immune infiltrate by IHC. CD3, CD8, and FoxP3 levels were noted to be higher in treatment-naïve metastatic tumors than in primary UM tumors. Consistent with prior work, PD-L1 expression was absent in 66.4% of primary tumors and 100% of treatment-naïve metastatic tumors. Where present in primary tumors, PD-L1 expression was <1%. In metastatic tumors, we noted no difference in immune infiltrate by metastatic site, pre-treatment and post-treatment time points, and in response to immunotherapy versus targeted therapy. NanoString analysis in a small cohort of patients treated with immunotherapy revealed an IFN-γ signature in the pre-treatment metastatic tumors of R compared with NR. *SOCS1* and HLA molecules were also significantly higher in pre-treatment tumors from R versus NR. The pre-treatment tumors of NR showed a gene expression profile consistent with a pro-inflammatory signaling network.

The success of immune checkpoint blockade in CM has relied heavily on the potency of the anti-tumor immune response, attributed mainly to the capacity of CD8+ lymphocytes to infiltrate and lyse tumors on an antigen-specific basis.[19] However, clinical response rates to anti-CTLA-4 and anti-PD-1 checkpoint blockade have been largely unimpressive (0 to 10%) with no benefit in terms of OS in UM.[9 10] One report of a small cohort of 15 UM patients treated with combinational checkpoint inhibitors showed that partial response was observed only in two cases, and the median of progression-free survival) was 2.8 months.[20] The reasons underlying the poor response to immunotherapy in UM are unclear. One explanation for this is the notable difference in the mutation burden between CM and UM. UM has been shown to present a limited mutational load compared with CM, which may contribute to low tumor immunogenicity in UM.[4 5] Another unifying explanation for the distinctive immune resistance of UMs is the anatomic site in which it arises. First, the eye is an immune-privileged site, which serves to limit the amount of immune-mediated inflammation occurring in this vital organ because its capacity to regenerate tissue is limited.[21 22] Second, the eye lacks lymphatic drainage, thus promoting retention of tumor antigens in the ocular environment without presentation to draining lymph nodes and the subsequent generation of a typical cell-based immune response.[23 24] Likewise, metastatic foci may themselves have evolved from their primary UM counterparts and may carry with them intrinsic mechanisms to evade immune surveillance.

There is limited literature on the immune signature of metastatic UM tumors.[13 25–27] Most UM metastases are collected via biopsy. Thus, it is difficult to collect adequate tissue from which to study an immune profile and gene signatures. Our previous study showed that the CD8+ T cells levels were significantly higher in CM metastases than UM metastases.[13] In this study, we once again demonstrate that UM tumors have an immune infiltrate

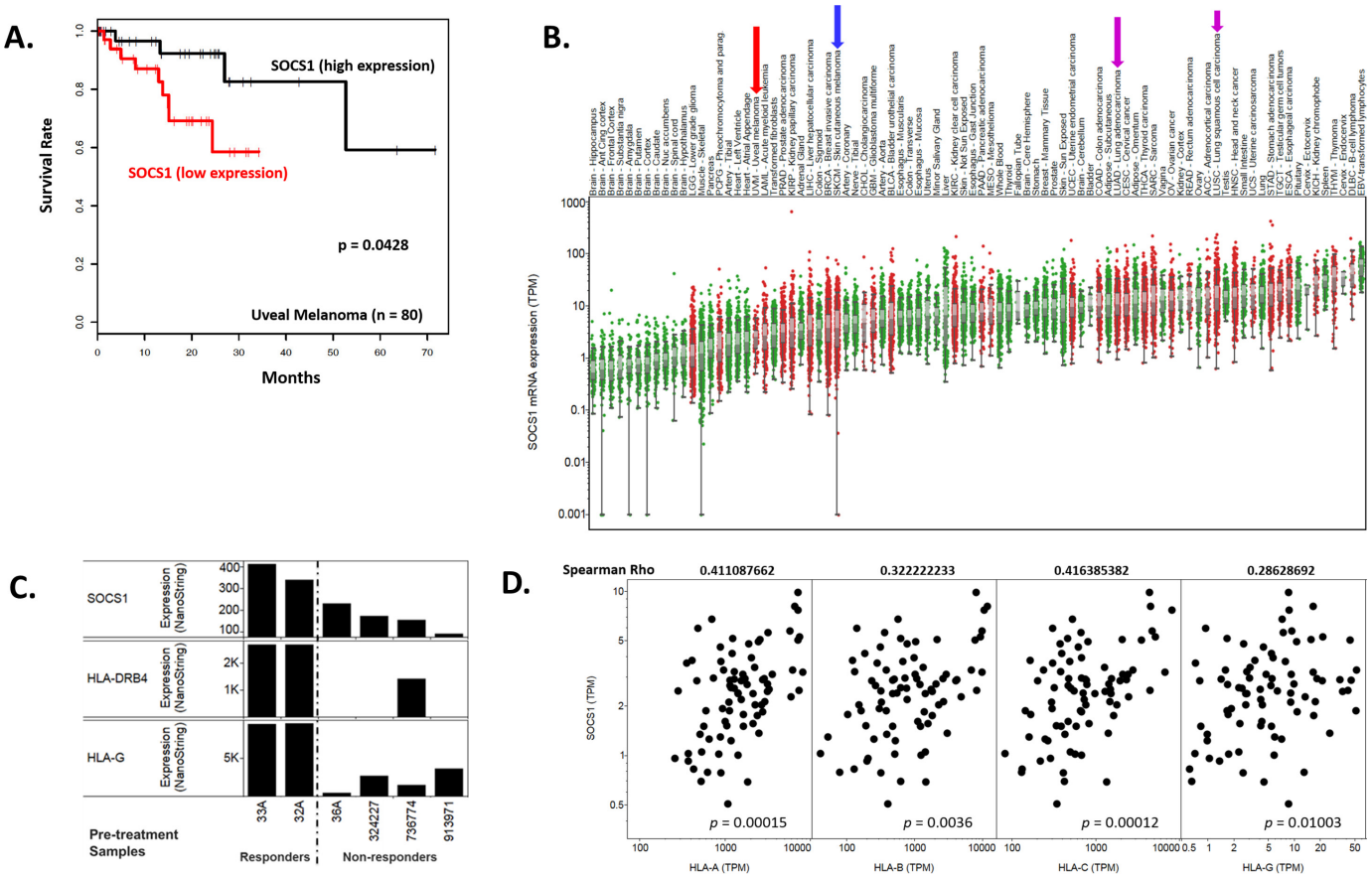

Figure 5 SOCS1 related signature in uveal melanoma (UM) tumors. (A) The Kaplan-Meier survival analysis of 80 primary UM tumors in The Cancer Genome Atlas (TCGA) showed that patients with low expression of SOCS1 (<medium, red line) had a statistically lower survival rate than in those with high expression of SOCS1 (>medium, black line). p=0.0428. (B) SOCS1 mRNA levels in various tumors (red dots) and normal tissues (green dots) based on based on TCGA and Genotype-Tissue expression (GTEx) data. SOCS1 in UM (red arrows) is significantly lower than cutaneous melanoma (CM; blue arrow), lung adenocarcinoma, and lung squamous cell carcinoma (purple arrows). (C) Comparison of SOCS1, human leukocyte antigen (HLA)-DRB4, and HLA-G expression levels in pretreatment UM tumors of responders versus non-responders who received immunotherapies. The mRNA levels of these three genes were determined by NanoString nCounter platform. (D) Dot plots from TCGA data of 80 UM tumors for the correlations of *SOTS1* levels and the expressions of several HLA genes. The significant correlations of gene expressions as measured by RNA-seq of TCGA are shown (p≤0.05).

and are not an immune desert. UM metastases contain CD3+, CD8+, CD4+, CD68+, and FoxP3+ infiltrates at higher levels than primary UM. These studies suggest the presence of immune suppressive mechanisms leading to the inactivation of T cells within metastatic UM tumors despite a population of intratumoral CD8+ and CD4+ infiltrates.

A study from Coupland's group showed that CD68+ and CD163+ tumor-associated macrophages were seen in all tested UM metastases.[26] In their study, CD3+ TILs were noted both within metastatic UMs and surrounding the tumor. CD8+ TILs were few in number within metastatic UMs but were predominantly seen peritumorally at the interface of tumor and normal liver, whereas CD4+ TIL showed a high perivascular density within metastatic UMs. In our study, most of the tested primary (92.6%) and metastatic UM (75% to 79%) tumors had intratumoral CD8+ infiltrates, and the presence of peritumoral immune infiltrates was only detected in a small portion of tumors. The definition of intratumoral and peritumoral infiltrates may be dependent on the quality of tissue specimens. Sufficient surrounding normal tissue in a tumor biopsy could be a critical factor in accurately describing the location of immune infiltrates.

Several studies have indicated that tumor-infiltrating CD4+CD25+FoxP3+Tregs are associated with decreased survival of various malignancies.[28–31] Tregs can suppress proliferation, cytokine production, and cytolytic activity of CD4+ and CD8+ T cells by mechanisms involving cell-to-cell contact and the release of cytokines, such as TGF-β.[32 33] Tregs can also induce an immunosuppressive phenotype in other cell types such as macrophages.[32–34] Our analysis found that FoxP3+ infiltrates in UM tumors were positively associated with CD3+ and CD8+ infiltrates (online supplemental figure S2A,B). These findings provide insight into the potential immune resistance mechanisms of UM.

Notably, our study again showed that the PD-1 and PD-L1 expression levels are low to absent in UMs as confirmed by previous studies.[13 27] PD-1 expression is

Table 2 Correlations of SOCS1 levels and the expressions of HLA molecules in 80 UM tumors from TCGA data

Gene_1	Gene_2	Spearman Rho	P value
SOCS1	HLA-A	0.411087662	0.000151916
SOCS1	HLA-B	0.322222233	0.003558534
SOCS1	HLA-C	0.416385382	0.000122208
SOCS1	HLA-DMA	0.322456628	0.003533064
SOCS1	HLA-DMB	0.356704175	0.001163051
SOCS1	HLA-DOA	0.397702754	0.000259111
SOCS1	HLA-DOB	0.293287873	0.008283405
SOCS1	HLA-DPA1	0.368026257	0.00078332
SOCS1	HLA-DPB1	0.365002334	0.000871762
SOCS1	HLA-DPB2	0.357601017	0.001127789
SOCS1	HLA-DQA1	0.31701827	0.004167862
SOCS1	HLA-DQA2	0.200164095	0.075041885
SOCS1	HLA-DQB1	0.329653084	0.002826087
SOCS1	HLA-DQB2	0.357949644	0.001114345
SOCS1	HLA-DRA	0.367557436	0.000796474
SOCS1	HLA-DRB1	0.365260184	0.000863881
SOCS1	HLA-DRB5	0.248640418	0.026151334
SOCS1	HLA-DRB6	0.286404133	0.010007918
SOCS1	HLA-E	0.262376934	0.018713555
SOCS1	HLA-F	0.312494129	0.004771237
SOCS1	HLA-G	0.28628692	0.010039812
SOCS1	HLA-H	0.402086258	0.000218081
SOCS1	HLA-J	0.19507736	0.082906384
SOCS1	HLA-L	0.216010317	0.054300283
SOCS1	IFNG	0.301690549	0.006535861
SOCS1	SOCS1	1	0

HLA, human leukocyte antigen; SOC1, suppressor of cytokine signaling 1; TCGA, The Cancer Genome Atlas; UM, uveal melanoma.

known to increase in the activated CD8 T cells and acts as a negative feedback system for attenuating immune responses and an indicator of T cell exhaustion. The absence of PD-L1 expression on UM tumors may provide a rationale for the failure of anti-PD-1 monotherapy and suggests that immune resistance in UM may occur via alternate mechanisms.

While the clinical benefit to checkpoint blockade is low in UM, there is a small subset of R to this treatment class. Due to the low clinical response rate of UM to immunotherapy, there is limited research identifying biological signatures correlated with R versus NR. In a pilot study analyzing one UM responder's tumor tissue to anti-PD-1 therapy, Stern's group identified that germline MBD4 mutation might correlate with response to immune checkpoint inhibitor;[35 36] this data needs to be validated in a larger cohort of UM patients. Our data set lacked normal blood or tissue in which to confirm this finding. What we did have, however, was a pilot set of six immunotherapy-treated patients with matched pre-treatment and post-treatment tissues, on which we performed gene expression analysis to identify signatures correlating with R and NR. One gene of note in our study was *SOCS1*. Our analysis showed that the mRNA levels of *SOCS1* were significantly higher in R compared with NR.

SOCS1 is a negative regulator of cytokine signal transduction, which suppresses cellular responses to various cytokines, including IFNs, interleukin (IL)-6, IL-4, leukemia inhibitory factor, growth hormones, and oncostatin M.[37] *SOCS1* suppresses cytokine signaling by directly binding to active Janus kinases (JAKs) through the SH2 domain resulting in blocked phosphorylation and inactivation of the JAK-STAT pathway.[38] Opposing accumulated data showed that *SOCS1* negatively regulated IFN-γ and IL-12 signaling and acted as a checkpoint molecule for anti-tumor immunity.[39] For example, immunization with *SOCS1−/−* dendritic cells induces a hyper Th1 immune response, lupus-like autoimmune disease, and anti-tumor activity.[40] In *SOCS1*-knockout mice, the number of cytotoxic T lymphocytes increased with a higher response to IL-17 and IL-15.[41 42] Various in vivo studies showed that deletion or suppression of *SOCS1* in either myeloid cells or T cells enhanced anti-tumor immunity.[39] Thus, *SOCS1* was also proposed as an immune checkpoint for developing novel immunotherapy. Although the functions of *SOCS1* in tumors are controversial in various reports, these discrepancies might rely on different roles of *SOCS1* in a cell context-dependent manner within tumors. Therefore, it is crucial to characterize the *SOCS1* function and its expression status in UM tumors precisely, and we propose to do this in future studies.

It is known that the expression of *SOCS1* can be induced by various cytokines, including IL2, IL3, erythropoietin, granulocyte-macrophage colony stimulating factor, and IFN-γ.[43] A couple of studies showed that *SOCS1* gene methylation and histone H3K9 methylation caused gene silencing of *SOCS1* in myeloid leukemia cells.[44 45] However, the underlying mechanism of suppressing *SOCS1* expression in UM remains unknown. The modulation of *SOCS1* levels could influence IFN responsiveness in the melanoma cell lines with artificial *SOCS1* overexpression by transfecting plasmid constructs.[46] Several small agents, such as chaetocin (histone methyltransferase inhibitor) and CDM-3008 (IFN-like small chemical compound), could enhance *SOCS1* expression in normal tissue and cancer cells.[45 47] These agents' potential to induce *SOCS1* expression and improve efficacy to checkpoint inhibitors in unresponsive tumors such as UM requires additional evaluation. Further studies are also needed to validate whether the high expression of *SOCS1* represents a normal functional feedback regulation of IFN in UM cells.

Our study is the first of its kind to describe the immune infiltrate in a large dataset of primary and metastatic UM tumors, in metastatic tumors by anatomic location and changes in infiltrates after monotherapy checkpoint

blockade or targeted therapy. We describe a higher overall immune infiltrate in metastatic UM compared with primary UM, perhaps explained by the immune privilege in the eye, and no difference in immune cells by the metastatic sites. The immune infiltrates in metastatic tissues after monotherapy checkpoint blockade were numerically higher than after targeted therapy, without statistical significance in part due to the sample size of this analysis. Most notably, IFN-γ is noted to be the major upstream regulator for a group of genes (*CASP3, CDH1, HLA-G, IFITM2, SLAMF1, SOCS1, TLR3, and ATF1*) expressed at a significantly higher level in the pre-treatment tumors of patients responding to immunotherapy. Though the fraction of UM responders to immunotherapy is low, this finding suggests there may be a baseline tumor signature indicative of response, which may be used to identify appropriate patients for this class of treatment, while sparing those without the signature unnecessary toxicity. Some limitations of our NanoString data include the small sample size and the variety of checkpoint inhibitors used for treatment. In particular, the R (n=2) both received combination immunotherapy while NR (n=4) were all monotherapy patients. Nevertheless, the suggestion of a pre-treatment tumor gene signature in R versus NR is being validated in a larger combined data set of nivolumab plus ipilimumab clinical trial patients from the GEM1402 study (Spain) and the CA184-187 study (USA). The findings from this validation study will help us understand further resistance and response mechanisms of metastatic UM to immunotherapy.

CONCLUSION

Our study, for the first time, demonstrates that patients with metastatic UM tumors have significantly higher levels of an immune infiltrate (CD3+, CD8+, FoxP3+, and CD68+ cells) compared with patients with primary UM tumors. We confirm that PD-1 and PD-L1 expression were low to absent in both groups. Furthermore, the presence of a baseline IFN-γ gene signature, specifically upregulation of the SOCS1 gene, was identified as a predictive marker for response to checkpoint blockade in our patient cohort, whereas the presence of a pro-inflammatory signature was predictive of non-response. Given the low response to checkpoint blockade immunotherapy in UM, our work provides insight into the differences in tumor-infiltrating immune cells and gene signatures between responders and non-responders in pre-treatment tissue. This work is being validated in a larger data set of patient tumors and may help inform therapeutic decision-making in the clinical setting.

Author affiliations
[1]Pharmaceutical Sciences, School of Pharmacy, The University of Texas at El Paso, El Paso, Texas, USA
[2]Medical Oncology, Scripps MD Anderson Cancer Center, San Diego, California, USA
[3]Translational Molecular Pathology, University of Texas MD Anderson Cancer Center, Houston, Texas, USA
[4]Center for Melanoma Research and Treatment, California Pacific Medical Center Research Institute, San Francisco, California, USA
[5]Melanoma Medical Oncology, University of Texas MD Anderson Cancer Center, Houston, Texas, USA
[6]Thoracic/Head & Neck Medical Oncology, University of Texas MD Anderson Cancer Center, Houston, Texas, USA
[7]Neurology, University of Texas Health Science Center at Houston, Houston, Texas, USA
[8]Department of Pathology, University of Texas MD Anderson Cancer Center, Houston, Texas, USA
[9]Department of Head and Neck Surgery, Section of Ophthalmology, University of Texas MD Anderson Cancer Center, Houston, Texas, USA
[10]Orbital Oncology & Ophthalmic Plastic Surgery, Department of Plastic Surgery, University of Texas MD Anderson Cancer Center, Houston, Texas, USA

Correction notice This article has been corrected since it was first published to update the funding statement.

Twitter Sapna P Patel @DrSapnaPatel

Acknowledgements We thank the MD Anderson Departments of Melanoma Medical Oncology and Division of Pathology for their resources and support. We would like to acknowledge Dr Gregory A Daniels for his contribution in mentorship and early phase of study conceptualization with Dr Bollin. A special acknowledgment to Dr Jennifer Wargo and Dr Zachary Cooper for their review of grant applications for this project. We also thank the Scripps Clinic Bio-Repository, and both Bethany Barrick and Dr Jamie Case for their assistance in providing us with some of the samples used in this study.

Contributors SP administered and supervised the project. SP, YQ, and KB conceptualized the work, contributed to funding acquisition, analyzed the data, and wrote the manuscript. MPdM and FC performed immunohistochemistry with oversight from MTT, W-LW, and AJL. SP, KB and KBK contributed patient samples. JR performed statistical analysis and graphical outputs. STR and YQ performed data collection. KMW and AR developed and executed methodology for the experimental studies. All authors read, edited, and approved the final manuscript.

Funding This work was supported by the National Institutes of Health/National Cancer Institute Cancer Center Support Grant under award number P30CA016672 and used the Tissue Biospecimen and Pathology Resource. This work was also supported by the MD Anderson Institutional Research Grant Award #40080 (principal investigator: SP Patel) and an NIH R21 award number 1R21CA208609 (principal investigator SP Patel). A Reuben is supported by the Kimberley Clarke Foundation Award for Scientific Achievement provided by MD Anderson's Odyssey Fellowship program.

Competing interests SP reports personal fees from Merck & Co, Incyte, Castle Biosciences, and Cardinal Health, and institutional clinical trial support from Provectus, Ideaya, and Bristol Myers Squibb outside the submitted work.

Patient consent for publication Not required.

Provenance and peer review Not commissioned; externally peer-reviewed.

Data availability statement All data relevant to the study are included in the article or uploaded as supplementary information.

ORCID iDs
Yong Qin http://orcid.org/0000-0003-4743-938X
Patrick Hwu http://orcid.org/0000-0003-0554-2856
Sapna P Patel http://orcid.org/0000-0003-1339-1517

REFERENCES

1 Patel SP. Latest developments in the biology and management of uveal melanoma. *Curr Oncol Rep* 2013;15:509–16.
2 Colombino M, Capone M, Lissia A, *et al*. BRAF/NRAS mutation frequencies among primary tumors and metastases in patients with melanoma. *J Clin Oncol* 2012;30:2522–9.
3 Van Raamsdonk CD, Bezrookove V, Green G, *et al*. Frequent somatic mutations of GNAQ in uveal melanoma and blue naevi. *Nature* 2009;457:599–602.
4 Furney SJ, Pedersen M, Gentien D, *et al*. Sf3B1 mutations are associated with alternative splicing in uveal melanoma. *Cancer Discov* 2013;3:1122–9.
5 Snyder A, Makarov V, Merghoub T, *et al*. Genetic basis for clinical response to CTLA-4 blockade in melanoma. *N Engl J Med* 2014;371:2189–99.
6 Chattopadhyay C, Kim DW, Gombos DS, *et al*. Uveal melanoma: from diagnosis to treatment and the science in between. *Cancer* 2016;122:2299–312.
7 Rapisuwon S, Qin Y, Roszik J. Systemic therapy for mucosal, acral and uveal melanoma. In: Balch C, ed. *Cutaneous melanoma*. Springer, Cham, 2019.
8 Carvajal RD, Piperno-Neumann S, Kapiteijn E, *et al*. Selumetinib in combination with dacarbazine in patients with metastatic uveal melanoma: a phase III, multicenter, randomized trial (SUMIT). *J Clin Oncol* 2018;36:1232–9.
9 Zimmer L, Vaubel J, Mohr P, *et al*. Phase II DeCOG-study of ipilimumab in pretreated and treatment-naïve patients with metastatic uveal melanoma. *PLoS One* 2015;10:e0118564.
10 Luke JJ, Callahan MK, Postow MA, *et al*. Clinical activity of ipilimumab for metastatic uveal melanoma: a retrospective review of the Dana-Farber cancer Institute, Massachusetts General Hospital, Memorial Sloan-Kettering cancer center, and university hospital of Lausanne experience. *Cancer* 2013;119:3687–95.
11 Algazi AP, Tsai KK, Shoushtari AN, *et al*. Clinical outcomes in metastatic uveal melanoma treated with PD-1 and PD-L1 antibodies. *Cancer* 2016;122:3344–53.
12 Mahoney KM, Freeman GJ, McDermott DF. The next Immune-Checkpoint inhibitors: PD-1/PD-L1 blockade in melanoma. *Clin Ther* 2015;37:764–82.
13 Qin Y, Petaccia de Macedo M, Reuben A, *et al*. Parallel profiling of immune infiltrate subsets in uveal melanoma versus cutaneous melanoma unveils similarities and differences: a pilot study. *Oncoimmunology* 2017;6:e1321187.
14 Hugo W, Zaretsky JM, Sun L, *et al*. Genomic and transcriptomic features of response to anti-PD-1 therapy in metastatic melanoma. *Cell* 2016;165:35–44.
15 Johansen LL, Lock-Andersen J, Hviid TVF. The pathophysiological impact of HLA class Ia and HLA-G expression and regulatory T cells in malignant melanoma: a review. *J Immunol Res* 2016;2016:1–11.
16 Ilangumaran S, Finan D, La Rose J, *et al*. A positive regulatory role for suppressor of cytokine signaling 1 in IFN-gamma-induced MHC class II expression in fibroblasts. *J Immunol* 2002;169:5010–20.
17 Rodríguez T, Méndez R, Del Campo A, *et al*. Distinct mechanisms of loss of IFN-gamma mediated HLA class I inducibility in two melanoma cell lines. *BMC Cancer* 2007;7:34.
18 Ilangumaran S, Rottapel R. Regulation of cytokine receptor signaling by SOCS1. *Immunol Rev* 2003;192:196–211.
19 Gros A, Robbins PF, Yao X, *et al*. Pd-1 identifies the patient-specific $CD8^+$ tumor-reactive repertoire infiltrating human tumors. *J Clin Invest* 2014;124:2246–59.
20 Heppt MV, Heinzerling L, Kähler KC, *et al*. Prognostic factors and outcomes in metastatic uveal melanoma treated with programmed cell death-1 or combined PD-1/cytotoxic T-lymphocyte antigen-4 inhibition. *Eur J Cancer* 2017;82:56–65.
21 Bronkhorst IHG, Jager MJ. Uveal melanoma: the inflammatory microenvironment. *J Innate Immun* 2012;4:454–62.
22 Niederkorn JY. Ocular immune privilege and ocular melanoma: parallel universes or immunological plagiarism? *Front Immunol* 2012;3:148.
23 Bronkhorst IHG, Vu THK, Jordanova ES, *et al*. Different subsets of tumor-infiltrating lymphocytes correlate with macrophage influx and monosomy 3 in uveal melanoma. *Invest Ophthalmol Vis Sci* 2012;53:5370–8.
24 Jia R, Jiao Z, Xu X, *et al*. Functional significance of B7-H1 expressed by human uveal melanoma cells. *Mol Med Rep* 2011;4:163–7.
25 Rothermel LD, Sabesan AC, Stephens DJ, *et al*. Identification of an immunogenic subset of metastatic uveal melanoma. *Clin Cancer Res* 2016;22:2237–49.
26 Krishna Y, McCarthy C, Kalirai H, *et al*. Inflammatory cell infiltrates in advanced metastatic uveal melanoma. *Hum Pathol* 2017;66:159–66.
27 Javed A, Arguello D, Johnston C, *et al*. Pd-L1 expression in tumor metastasis is different between uveal melanoma and cutaneous melanoma. *Immunotherapy* 2017;9:1323–30.
28 Siddiqui SA, Frigola X, Bonne-Annee S, *et al*. Tumor-Infiltrating Foxp3-CD4+CD25+ T cells predict poor survival in renal cell carcinoma. *Clin Cancer Res* 2007;13:2075–81.
29 Li F, Guo Z, Lizée G, *et al*. Clinical prognostic value of CD4+CD25+FOXP3+regulatory T cells in peripheral blood of Barcelona clinic liver cancer (BCLC) stage B hepatocellular carcinoma patients. *Clin Chem Lab Med* 2014;52:1357–65.
30 Tang Y, Xu X, Guo S, *et al*. An increased abundance of tumor-infiltrating regulatory T cells is correlated with the progression and prognosis of pancreatic ductal adenocarcinoma. *PLoS One* 2014;9:e91551.
31 Preston CC, Maurer MJ, Oberg AL, *et al*. The ratios of CD8+ T cells to CD4+CD25+ Foxp3+ and FOXP3- T cells correlate with poor clinical outcome in human serous ovarian cancer. *PLoS One* 2013;8:e80063.
32 Milne K, Köbel M, Kalloger SE, *et al*. Systematic analysis of immune infiltrates in high-grade serous ovarian cancer reveals CD20, FOXP3 and TIA-1 as positive prognostic factors. *PLoS One* 2009;4:e6412.
33 Miyara M, Sakaguchi S. Natural regulatory T cells: mechanisms of suppression. *Trends Mol Med* 2007;13:108–16.
34 Cassetta L, Kitamura T. Targeting tumor-associated macrophages as a potential strategy to enhance the response to immune checkpoint inhibitors. *Front Cell Dev Biol* 2018;6:38.
35 Rodrigues M, Mobuchon L, Houy A, *et al*. Outlier response to anti-PD1 in uveal melanoma reveals germline MBD4 mutations in hypermutated tumors. *Nat Commun* 2018;9:1866.
36 Johansson PA, Stark A, Palmer JM, *et al*. Prolonged stable disease in a uveal melanoma patient with germline MBD4 nonsense mutation treated with pembrolizumab and ipilimumab. *Immunogenetics* 2019;71:433–6.
37 Inagaki-Ohara K, Kondo T, Ito M, *et al*. Socs, inflammation, and cancer. *JAKSTAT* 2013;2:e24053.
38 Croker BA, Kiu H, Nicholson SE. Socs regulation of the JAK/STAT signalling pathway. *Semin Cell Dev Biol* 2008;19:414–22.
39 Chikuma S, Kanamori M, Mise-Omata S, *et al*. Suppressors of cytokine signaling: potential immune checkpoint molecules for cancer immunotherapy. *Cancer Sci* 2017;108:574–80.
40 Hanada T, Tanaka K, Matsumura Y, *et al*. Induction of hyper Th1 cell-type immune responses by dendritic cells lacking the suppressor of cytokine signaling-1 gene. *J Immunol* 2005;174:4325–32.
41 Chong MMW, Cornish AL, Darwiche R, *et al*. Suppressor of cytokine signaling-1 is a critical regulator of interleukin-7-dependent CD8+ T cell differentiation. *Immunity* 2003;18:475–87.
42 Davey GM, Starr R, Cornish AL, *et al*. Socs-1 regulates IL-15-driven homeostatic proliferation of antigen-naive CD8 T cells, limiting their autoimmune potential. *J Exp Med* 2005;202:1099–108.
43 Krebs DL, Hilton DJ. Socs: physiological suppressors of cytokine signaling. *J Cell Sci* 2000;113 (Pt 16:2813–9.
44 Zhang X-H, Yang L, Liu X-J, *et al*. Association between methylation of tumor suppressor gene SOCS1 and acute myeloid leukemia. *Oncol Rep* 2018;40:1008–16.
45 Lee M-C, Kuo Y-Y, Chou W-C, *et al*. Gfi-1 is the transcriptional repressor of SOCS1 in acute myeloid leukemia cells. *J Leukoc Biol* 2014;95:105–15.
46 Lesinski GB, Zimmerer JM, Kreiner M, *et al*. Modulation of SOCS protein expression influences the interferon responsiveness of human melanoma cells. *BMC Cancer* 2010;10:142.
47 Furutani Y, Toguchi M, Shiozaki-Sato Y, *et al*. An interferon-like small chemical compound CDM-3008 suppresses hepatitis B virus through induction of interferon-stimulated genes. *PLoS One* 2019;14:e0216139.

Correction: *Immune profiling of uveal melanoma identifies a potential signature associated with response to immunotherapy*

Qin Y, Bollin K, de Macedo MP, *et al*. Immune profiling of uveal melanoma identifies a potential signature associated with response to immunotherapy. *J Immunother Cancer* 2020;**8:**e000960. doi:10.1136/jitc-2020-000960

This article has been corrected since it was first published. The following sentence has been added to the funding statement: '…and an NIH R21 award number 1R21CA208609 (principal investigator SP Patel).'

J Immunother Cancer 2022;**10**:e000960corr1. doi:10.1136/jitc-2020-000960corr1